

The Geometry of the Scroll Compressor*

Jens Gravesen[†]
Christian Henriksen[†]

Abstract. The scroll compressor is an ingenious machine used for compressing air or refrigerant; it was originally invented in 1905 by Léon Creux. The classical design consists of two nested identical scrolls given by circle involutes, one of which is rotated through 180° with respect to the other. By specifying not a parametrization of the curve, but instead the radius of curvature as a function of tangent direction and using the intrinsic equation of a planar curve, the design can be changed in a way that allows all relevant geometrical quantities to be calculated in closed analytical form.

Key words. scroll compressor, intrinsic equation, planar curves, tangent direction

AMS subject classifications. 53A04, 53A17, 00A69

PII. S0036144599362121

I. Introduction. The scroll compressor is an ingenious machine used for compressing air or refrigerant, which was originally invented in 1905 by Léon Creux [2]. At the time technology was insufficiently advanced for workable models to be manufactured, and it wasn't until the 1970s that commercial interest in the idea was revived; see, e.g., [7]. The device consists of two nested identical scrolls, one of which is rotated through 180° with respect to the other. In the classical design both scrolls are *circle involutes* as shown in Figure 1.1.

Today, scroll compressors are widely used for compressing refrigerants in air-conditioners. There are many advantages over the traditional piston-pump design. For example, only a small number of moving parts and no valves are required, and the rotary motion can be completely balanced, reducing vibration and noise.

One problem with the traditional design is that the compression takes place rather slowly, so a large number of turns is required to achieve the high compression demanded for refrigeration and freezing. Unfortunately, for a given total cross-sectional area, increasing the tightness of the spiral first decreases the choke volume of gas that can be ingested in each cycle, then makes the job of machining the scrolls more difficult, and finally increases the rate of leakage.

At the 32nd European Study Group with Industry held in September 1998 at the Technical University of Denmark, Stig Helmer Jørgensen from Danfoss A/S presented the problem of finding a better design for the scroll compressor.

There are at least two possible ways to change the compressor: the first is to change the geometry of the scrolls, and the second is to change the orbit of the

*Received by the editors October 1, 1999; accepted for publication (in revised form) August 9, 2000; published electronically February 2, 2001.

<http://www.siam.org/journals/sirev/43-1/36212.html>

[†]Department of Mathematics, Technical University of Denmark, Building 303, DK-2800 Lyngby, Denmark (J.Gravesen@mat.dtu.dk, Christian.Henriksen@mat.dtu.dk).

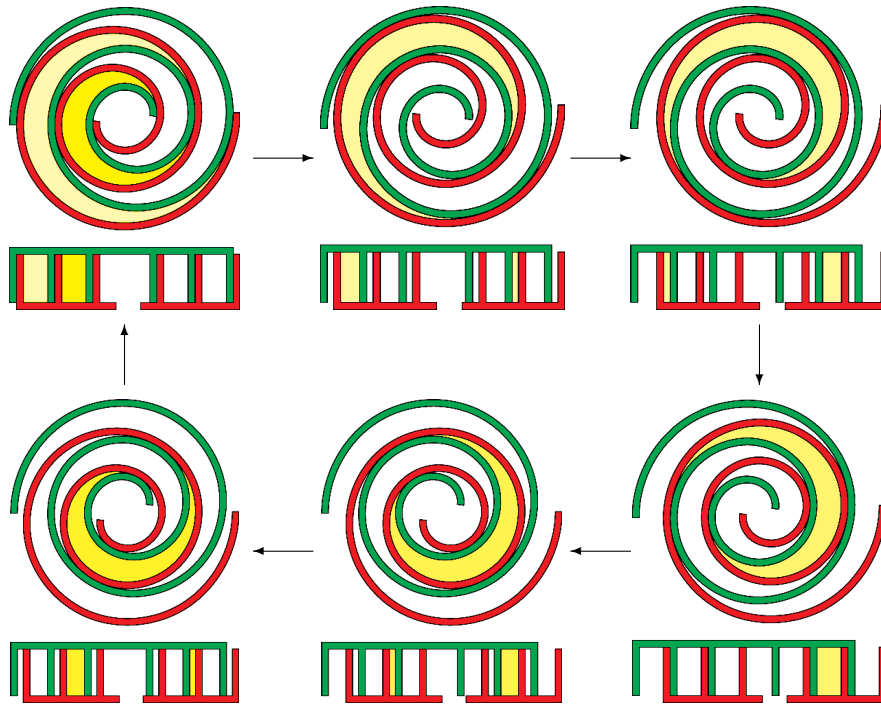


Fig. 1.1 Schematic diagram of a scroll compressor. While the red scroll is kept fixed, the green is orbiting in a circular movement, and this presses the yellow gas captured in the pockets towards the center of the compressor. In this diagram only one cycle is needed, but to our knowledge all commercial scroll compressors are made with one more turn and thus need two cycles to complete the compression.

motion. In this paper we will ignore the latter possibility and only consider changes to the geometry of the scrolls.

Ignoring the ends of the scroll, it is bounded by two planar curves, which are the objects we want to design. The inside of one scroll and the outside of the other form what we call a *mating pair* of sides. During the motion, two mating sides touch each other at a number of points bounding a sequence of compression chambers, and it is the volume of these chambers that determines the compression and choke volume. As in the classical design we will also let the two scrolls be identical and rotated through 180° . This implies that the two mating pairs of sides are identical too.

So we have the following procedure for the design of a scroll compressor:

- Design one side of the moving scroll.
- Determine the mating side on the fixed scroll as the envelope of the newly designed side of the moving scroll.
- Determine the other mating pair of sides by reflection in a suitable point.

Once this is done we have the following problems to solve:

- Ensure the geometric integrity of the design; i.e., the two scrolls must not overlap each other or themselves.
- Determine the geometric compression and choke volume; i.e., determine these two quantities assuming no leakage.

The goal is to combine the geometry with mechanical and fluid mechanical modeling and put all this into an optimization loop. This is currently being pursued in coop-

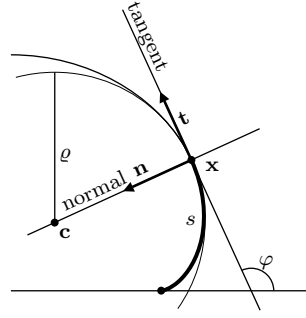


Fig. 2.1 Some basic geometric concepts: the arc-length s , the tangent direction φ , the radius of curvature $\varrho = ds/d\varphi$, and the center of curvature \mathbf{c} .

eration with Danfoss A/S, but in this paper we will be content with the geometrical modeling of the compressor. The key idea is to represent the curves defining the shape of the scroll compressor by the so-called *natural* or *intrinsic equation*. Doing this, all the relevant geometric quantities can be calculated in closed analytical form.

We should mention that besides the geometrical modeling of the compressor, fluid mechanical modeling was also done by the study group; see [4] and [6].

2. The Geometry of the Scroll Compressor. Commonly a planar curve is given by a parametrization $t \mapsto \mathbf{x}(t)$, but it might as well be given by its *intrinsic equation*, i.e., an equation that links the arc-length s and the tangent direction φ ; see Figure 2.1. We use the (simple) differential equation

$$(2.1) \quad \frac{ds}{d\varphi} = \varrho(\varphi),$$

where ϱ is the *radius of curvature*. In other words, we specify the radius of curvature as a function of tangent direction. We can then recapture the arc-length by

$$s = \int_0^\varphi \varrho(u) du.$$

We introduce the orthonormal frame

$$(2.2) \quad \mathbf{e}(\varphi) = (\cos \varphi, \sin \varphi) \quad \text{and} \quad \mathbf{f}(\varphi) = (-\sin \varphi, \cos \varphi).$$

By the definition of the tangent direction φ we have $\mathbf{t}(\varphi) = \mathbf{e}(\varphi)$. If $\mathbf{x}(\varphi)$ is the parametrization by tangent direction, then

$$\frac{d\mathbf{x}}{d\varphi} = \frac{ds}{d\varphi} \mathbf{t}(\varphi) = \varrho \mathbf{e}(\varphi),$$

and we can determine \mathbf{x} by integration

$$(2.3) \quad \mathbf{x}(\varphi) = \int_0^\varphi \varrho(u) \mathbf{e}(u) du = \int_0^\varphi (\varrho(u) \cos u, \varrho(u) \sin u) du.$$

Notice that both the arc-length s and the parametrization \mathbf{x} can be determined in closed form if $\varrho(\varphi)$ is a polynomial or just a piecewise polynomial in φ , and that the parametrization is by tangent direction.

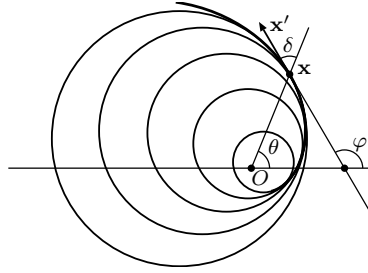


Fig. 2.2 The angle θ increases if the origin O is to the left of the tangent.

It is important to ensure that the curve is without self-intersection and that it is a spiral. The following classical result shows that the latter is the case if ϱ is a strictly increasing positive function.

THEOREM 2.1 (Kneser's theorem). *Let \mathbf{x} be a curve, given by the intrinsic equation $\varrho = \varrho(\varphi)$. Let $\mathbf{c}(\varphi)$ be the evolute (i.e., the locus of the center of curvature) for \mathbf{x} , let D_φ be the open disk bounded by the circle of curvature,*

$$D_\varphi = \{\mathbf{p} \in \mathbb{R}^2 \mid |\mathbf{p} - \mathbf{c}(\varphi)| < \varrho(\varphi)\},$$

and let \overline{D}_φ be the closure of D_φ . If $\varrho(\varphi)$ is a strictly increasing positive function, then the disks D_φ form a strictly increasing sequence,

$$(2.4) \quad \varphi_1 < \varphi_2 \Rightarrow \overline{D}_{\varphi_1} \subset D_{\varphi_2},$$

and the curve passes from the inside to the outside of each disk,

$$(2.5) \quad \varphi_1 < \varphi_2 \Rightarrow \mathbf{x}(\varphi_1) \in D_{\varphi_2} \quad \text{and} \quad \mathbf{x}(\varphi_2) \notin \overline{D}_{\varphi_1}.$$

For the proof, see, e.g., [5, p. 48]. We furthermore have the following lemma.

LEMMA 2.2. *With the same assumptions as in Kneser's theorem above, choose the origin $O \in \bigcap_\varphi \overline{D}_\varphi$ and let (r, θ) denote polar coordinates. Then the angle θ is a strictly increasing function of φ .*

Proof. Consider Figure 2.2; if the angle $\delta = \varphi - \theta$ between the vector $\mathbf{x} = \overrightarrow{OP}$ and the velocity vector \mathbf{x}' is in the interval $(0, \pi)$, then $\theta' > 0$. This is the case if O is to the left of \mathbf{x}' . As $\varrho' > 0$ the circle of curvature is to the left of \mathbf{x}' , and as O is inside any circle of curvature the proof is complete. \square

If in Kneser's theorem we replace the osculating circle with the *supporting half-plane*

$$(2.6) \quad H_\varphi = \{\mathbf{p} \in \mathbb{R}^2 \mid (\mathbf{p} - \mathbf{x}(\varphi)) \cdot \mathbf{f}(\varphi) \geq 0\},$$

then we have the following lemma.

LEMMA 2.3. *Let \mathbf{x} and ϱ be as in Kneser's theorem above; then*

$$\varphi \leq \varphi_0 + \pi \Rightarrow \mathbf{x}(\varphi) \in H_{\varphi_0}.$$

Proof. Observe that the osculating circle is contained in the supporting half-plane, so if $\varphi \leq \varphi_0$, the conclusion follows from Kneser's theorem. If $\varphi = \varphi_0 + \varphi_1$ and

$\varphi_1 \in [0, \pi]$, then we have

$$(2.7) \quad (\mathbf{x}(\varphi) - \mathbf{x}(\varphi_0)) \cdot \mathbf{f}(\varphi_0) = \int_0^{\varphi_1} \mathbf{x}'(\varphi_0 + u) \cdot \mathbf{f}(\varphi_0) \, du \\ = \int_0^{\varphi_1} \varrho(\varphi_0 + u) \mathbf{e}(\varphi_0 + u) \cdot \mathbf{f}(\varphi_0) \, du = \int_0^{\varphi_1} \varrho(\varphi_0 + u) \sin u \, du \geq 0,$$

because ϱ is positive. \square

We will later need the following lemma.

LEMMA 2.4. *Let \mathbf{x} and ϱ be as in Kneser's theorem above; then*

$$(\mathbf{x}(\varphi + 2n\pi) - \mathbf{x}(\varphi)) \cdot \mathbf{f}(\varphi) \leq 0 \quad \text{for all } n \in \mathbb{N},$$

$$(\mathbf{x}(\varphi + (2n + 1)\pi) - \mathbf{x}(\varphi)) \cdot \mathbf{f}(\varphi) \geq 0 \quad \text{for all } n \in \mathbb{N}.$$

Proof. As ϱ is increasing and positive we have

$$(\mathbf{x}(\varphi + 2\pi) - \mathbf{x}(\varphi)) \cdot \mathbf{f}(\varphi) = \int_0^{2\pi} \mathbf{x}'(\varphi + u) \cdot \mathbf{f}(\varphi) \, du \\ = \int_0^{2\pi} \varrho(\varphi + u) \mathbf{e}(\varphi + u) \cdot \mathbf{f}(\varphi) \, du = \int_0^{2\pi} \varrho(\varphi + u) \sin u \, du \leq 0,$$

which gives the first inequality. Similarly, by (2.7) and as

$$(\mathbf{x}(\varphi + 3\pi) - \mathbf{x}(\varphi + \pi)) \cdot \mathbf{f}(\varphi) = -(\mathbf{x}(\varphi + 3\pi) - \mathbf{x}(\varphi + \pi)) \cdot \mathbf{f}(\varphi + \pi) \geq 0,$$

we obtain the second inequality. \square

REMARK 2.5. *The increase of ϱ need not be strict for Lemmas 2.3 and 2.4 to hold. In other words, if ϱ is an increasing positive function of φ , then the lemmas hold.*

We now translate the curve \mathbf{x} in a circular orbit with radius r . That is, at time t we have the translated curve $\mathbf{x}_t(\varphi) = \mathbf{x}(\varphi) + \mathbf{d}(t)$. If we put $\mathbf{d}(t) = -r\mathbf{f}(t)$, then $\mathbf{d}'(t) = r\mathbf{e}(t)$ and \mathbf{d} describes a circular orbit parametrized by tangent direction. At time t the side \mathbf{x}_t of the moving scroll and the mating side \mathbf{y} of the fixed scroll touch each other at some points, so \mathbf{y} is an *envelope* of the family $\{\mathbf{x}_t \mid t \in \mathbb{R}\}$. If \mathbf{y} at time t touches \mathbf{x}_t at the point $\mathbf{x}_t(\varphi(t))$, then we can parametrize \mathbf{y} as

$$\mathbf{y}(t) = \mathbf{x}_t(\varphi(t)) = \mathbf{x}(\varphi(t)) + \mathbf{d}(t).$$

As \mathbf{x}_t and \mathbf{y} touch each other without crossing, their tangents are parallel; i.e., we have the condition $\mathbf{y}'(t) \parallel \mathbf{x}'_t(\varphi(t))$, or equivalently $\mathbf{d}'(t) \parallel \mathbf{x}'(\varphi(t))$. As φ is the tangent direction on \mathbf{x} and t is the tangent direction on \mathbf{d} we have

$$\varphi(t) = t + n\pi, \quad n \in \mathbb{Z}.$$

Note that in this case it is trivial to determine the function $\varphi(t)$, but if we don't use tangent direction as the parameter, then the equation determining $\varphi(t)$ is nonlinear and can generally only be solved numerically.

At first glance we seem to have an envelope \mathbf{y}_n for each $n \in \mathbb{Z}$, but as $\mathbf{d}(t)$ is periodic with period 2π we have $\mathbf{y}_{n+2}(t) = \mathbf{y}_n(t + 2\pi)$, so we have in fact only two different envelopes, one on each side of \mathbf{x}_t , which we write as

$$(2.8) \quad \mathbf{y}_+(t) = \mathbf{y}_0(t) = \mathbf{x}(t) + \mathbf{d}(t), \\ \mathbf{y}_-(t) = \mathbf{y}_1(t - \pi) = \mathbf{x}(t) - \mathbf{d}(t),$$

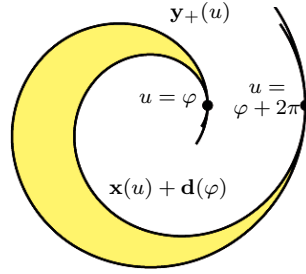


Fig. 3.1 The volume of a compressor chamber.

where we have used the fact that $\mathbf{d}(t - \pi) = -\mathbf{d}(t)$. This ensures that the envelopes are parametrized by tangent direction, i.e.,

$$\varphi_{\mathbf{y}_{\pm}} = \varphi_{\mathbf{x}} = \varphi_{\mathbf{d}} = \varphi,$$

where the subscript denotes the curve at hand. Differentiation of (2.8) yields

$$\mathbf{y}'_{\pm}(\varphi) = \mathbf{x}'(\varphi) \pm \mathbf{d}'(\varphi) = (\varrho \pm r)\mathbf{e}(\varphi),$$

and hence $\varrho_{\mathbf{y}_{\pm}} = \varrho_{\mathbf{x}} \pm r$. We have in particular that if $\varrho_{\mathbf{x}}$ is an increasing positive function, then so is $\varrho_{\mathbf{y}_{+}}$. So if we choose \mathbf{y}_{+} as the mating side of \mathbf{x} , then we avoid any problems of singularities on the mating fixed scroll.

3. The Volume of the Compression Chambers. The signed area between a pair \mathbf{u} and \mathbf{v} of planar vectors is given by the *planar product* or determinant of the pair, and we denote it $[\mathbf{u}, \mathbf{v}]$. A compression chamber is bounded by two curve segments (see Figure 3.1), and the area between the two segments on \mathbf{x} and \mathbf{y}_{+} is, by Green's formula, seen to be

$$\begin{aligned} \mathcal{A}(\varphi) &= \frac{1}{2} \int_{\varphi}^{\varphi+2\pi} \left([\mathbf{y}_{+}(u), \mathbf{y}'_{+}(u)] - [\mathbf{x}_{\varphi}(u), \mathbf{x}'_{\varphi}(u)] \right) du \\ &= \frac{1}{2} \int_{\varphi}^{\varphi+2\pi} \left([\mathbf{x}(u) + \mathbf{d}(u), \mathbf{y}'_{+}(u) + \mathbf{d}'(u)] - [\mathbf{x}(u) + \mathbf{d}(\varphi), \mathbf{x}'(u)] \right) du \\ (3.1) \quad &= \pi r^2 + r \left([\mathbf{x}(\varphi) - \mathbf{x}(\varphi + 2\pi), \mathbf{f}(\varphi)] + s_{\mathbf{x}}(\varphi + 2\pi) - s_{\mathbf{x}}(\varphi) \right). \end{aligned}$$

If we want three turns of the scrolls then φ has to run through an interval of length 6π , so we let $\varphi \in [0, 6\pi]$. If Δ_1 denotes the compression during the first cycle, Δ_2 denotes the compression during the second cycle, and Δ denotes the total compression, then we have

$$(3.2) \quad \Delta_1 = \frac{\mathcal{A}(4\pi)}{\mathcal{A}(2\pi)}, \quad \Delta_2 = \frac{\mathcal{A}(2\pi)}{\mathcal{A}(0)}, \quad \Delta = \Delta_1 \Delta_2 = \frac{\mathcal{A}(4\pi)}{\mathcal{A}(0)}.$$

4. Constant Wall Thickness. It seems natural to look for scrolls with constant wall thickness, which are characterized by the following simple result.

THEOREM 4.1. *Let \mathbf{x} and $\tilde{\mathbf{x}}$ be the sides of the moving scroll and let $\mathbf{y} = \mathbf{x} - r\mathbf{f}$ and $\tilde{\mathbf{y}} = \tilde{\mathbf{x}} + r\mathbf{f}$ be the corresponding mating sides of the fixed scroll. The scrolls have*

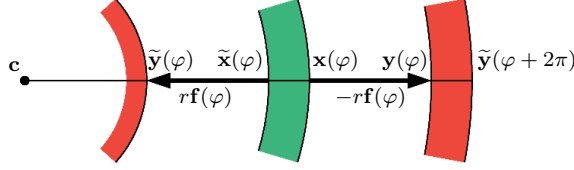


Fig. 4.1 Scrolls with constant width.

fixed width if and only if all four curves have a common simple, closed, and convex evolute.

Proof. The “if” part is trivial, so assume all four curves are parallel and thus have a common evolute \mathbf{c} . That the evolute is convex, i.e., has nonvanishing curvature, follows from the fact that the sides of the scrolls are smooth curves. So all we need to show is that the evolute is simple closed, i.e., that it is closed and without self-intersection.

If the widths of the two scrolls are δ_x and δ_y , respectively, then we have $\tilde{\mathbf{x}} = \mathbf{x} - \delta_x \mathbf{f}$ and $\tilde{\mathbf{y}}(\varphi + 2\pi) = \mathbf{y}(\varphi) + \delta_y \mathbf{f}(\varphi)$; see Figure 4.1. This implies that the two curves $\tilde{\mathbf{y}}$ and $\varphi \mapsto \tilde{\mathbf{y}}(\varphi + 2\pi)$ are parallel. Using once more the fact that parallel curves have a common evolute we see that $\mathbf{c}(\varphi) = \mathbf{c}(\varphi + 2\pi)$, so the common evolute is a closed curve. As $\varphi + \pi/2$ is the tangent direction on the evolute, it is periodic with period 2π when parametrized by tangent direction, but then it can’t have any self-intersections—in other words it is a simple curve. \square

Scrolls with constant width have a particular simple volume function. As \mathbf{x} is the evolute of \mathbf{c} , we have $\mathbf{x}(\varphi + 2\pi) - \mathbf{x}(\varphi) = -\ell_c \mathbf{f}(\varphi)$, where ℓ_c is the length of the closed evolute. So (3.1) reduces to

$$\mathcal{A}(\varphi) = \pi r^2 + r(s_{\mathbf{x}}(\varphi + 2\pi) - s_{\mathbf{x}}(\varphi)).$$

Furthermore, if we write $s_{\mathbf{c}}(\varphi) = \frac{\ell_c \varphi}{2\pi} + \bar{s}_{\mathbf{c}}(\varphi)$, then

$$\frac{d}{d\varphi} \int_{\varphi}^{\varphi+2\pi} \bar{s}_{\mathbf{c}}(u) du = \bar{s}_{\mathbf{c}}(\varphi + 2\pi) - \bar{s}_{\mathbf{c}}(\varphi) = s_{\mathbf{c}}(\varphi + 2\pi) - s_{\mathbf{c}}(\varphi) - \ell_c = 0,$$

and hence

$$\int_{\varphi}^{\varphi+2\pi} \bar{s}_{\mathbf{c}}(u) du = \int_0^{2\pi} \bar{s}_{\mathbf{c}}(u) du = \int_0^{2\pi} \left(s_{\mathbf{c}}(u) - \frac{\ell_c u}{2\pi} \right) du = \int_0^{2\pi} s_{\mathbf{c}}(u) du - \pi \ell_c.$$

As $s'_{\mathbf{x}}(\varphi) = \varrho_{\mathbf{x}}(\varphi) = \varrho_0 + s_{\mathbf{c}}(\varphi)$, we have

$$\begin{aligned} s_{\mathbf{x}}(\varphi + 2\pi) - s_{\mathbf{x}}(\varphi) &= \int_{\varphi}^{\varphi+2\pi} \left(\varrho_0 + \frac{\ell_c u}{2\pi} + \bar{s}_{\mathbf{c}}(u) \right) du \\ &= 2\pi \varrho_0 + \ell_c \varphi + \ell_c \pi + \int_0^{2\pi} s_{\mathbf{c}}(u) du - \pi \ell_c = 2\pi \varrho_0 + \int_0^{2\pi} s_{\mathbf{c}}(u) du + \ell_c \varphi, \end{aligned}$$

and the expression for the volume of the compression chamber finally reduces to

$$(4.1) \quad \mathcal{A}(\varphi) = \pi r^2 + 2\pi r \varrho_0 + r \int_0^{2\pi} s_{\mathbf{c}}(u) du + r \ell_c \varphi.$$

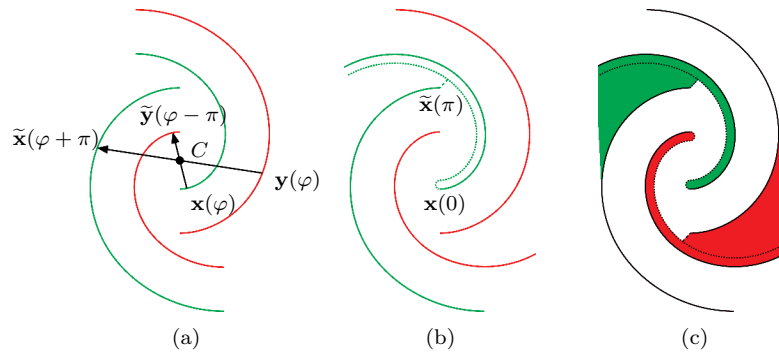


Fig. 5.1 (a) We reflect a pair of mating sides (\mathbf{x}, \mathbf{y}) in a point to get the other pair of mating sides $(\tilde{\mathbf{y}}, \tilde{\mathbf{x}})$. (b) The original (outer) side \mathbf{x} of the moving scroll is thickened on the inside by drawing a parallel curve (dotted), and the two parallel curves are connected by a half-circle. Then the end of the reflected image $\tilde{\mathbf{x}}$ of the original (inner) side \mathbf{y} of the fixed scroll is connected to the parallel dotted curve. Here we have just used a straight line segment (dashed), but in practice one could use a more smooth solution. (c) The construction is transferred to the fixed scroll by reflection and we have the two solid scrolls.

If we fix the length ℓ_c of the evolute, then the term that can affect the compression is $2\pi r \varrho_0 + r \int_0^{2\pi} s_c(u) du$. If we want a large compression, then this expression has to be as small as possible. In this paper we will not pursue scrolls with constant width any further, but will move on and consider more general designs.

5. The Other Side of the Scroll. So far we have in general only considered one pair of mating sides of the scrolls. We will now construct the two remaining sides by reflecting \mathbf{x} and \mathbf{y} in suitable chosen point C ; see Figure 5.1. Under the reflection we have

$$\mathbf{x}(\varphi) \mapsto \tilde{\mathbf{y}}(\varphi - \pi) \quad \text{and} \quad \mathbf{y}(\varphi) \mapsto \tilde{\mathbf{x}}(\varphi + \pi),$$

where \mathbf{x} and $\tilde{\mathbf{x}}$ are the sides of the moving scroll and \mathbf{y} and $\tilde{\mathbf{y}}$ are the sides of the fixed scroll. Observe that $\tilde{\mathbf{x}}$ and $\tilde{\mathbf{y}}$ are parametrized by tangent direction.

Somehow we have to connect the ends of \mathbf{x} to the ends of $\tilde{\mathbf{x}}$; the fixed scroll is then obtained by reflection in C . The outer end poses no problem, so we concentrate on connecting $\mathbf{x}(0)$ to $\tilde{\mathbf{x}}(\pi)$. We do this by attaching a small half-circle with radius δ to $\mathbf{x}(0)$, then continue back along a parallel curve to \mathbf{x} , and finally connect to $\tilde{\mathbf{x}}(\pi)$ along a straight line; see Figure 5.1. The connection from \mathbf{x} to $\tilde{\mathbf{x}}$ can of course be done in many other ways, and also in a more smooth way, but our simpleminded choice allows us an easy analysis of the intersection problem (cf. Theorem 5.1). To be more precise, if $\mathbf{x} : [0, \varphi_s] \rightarrow \mathbb{R}^2$, then we put $\mathbf{x}_\delta(\varphi) = \mathbf{x}(\varphi) + 2\delta\mathbf{f}(\varphi)$ and

$$(5.1) \quad \bar{\mathbf{x}}(\varphi) = \begin{cases} \mathbf{x}_\delta(-\varphi - \pi) & \text{if } \varphi \in [-\varphi_s - \pi, -\pi], \\ \mathbf{x}(0) + \delta(\mathbf{f}(0) - \mathbf{f}(\varphi)) & \text{if } \varphi \in [-\pi, 0], \\ \mathbf{x}(\varphi) & \text{if } \varphi \in [0, \varphi_s]. \end{cases}$$

Observe that the extension $\bar{\mathbf{x}}$ is parametrized by tangent direction too, and that the half-circle is $\mathbf{x}|_{[-\pi, 0]}$. To summarize the construction, we start with the radius of curvature of one side of the moving scroll, $\varrho_{\mathbf{x}} : [0, \varphi_s] \rightarrow \mathbb{R}$, and the radius of the circular orbit, $r \in \mathbb{R}$. Then we construct the side of the moving scroll $\mathbf{x} : [0, \varphi_s] \rightarrow \mathbb{R}^2$

and the side of the fixed scroll $\mathbf{y} = \mathbf{x} - r\mathbf{f} : [0, \varphi_s] \rightarrow \mathbb{R}^2$. By reflection we obtain the other sides $\tilde{\mathbf{x}} : [\pi, \varphi_s + \pi] \rightarrow \mathbb{R}^2$ and $\tilde{\mathbf{y}} : [-\pi, \varphi_s - \pi] \rightarrow \mathbb{R}^2$. We extend \mathbf{x} with a half-circle of radius δ as described above and obtain $\bar{\mathbf{x}} : [-\pi, \varphi_s] \rightarrow \mathbb{R}^2$. Still reflecting in C , we obtain an extension $\bar{\mathbf{y}}$ of $\tilde{\mathbf{y}}$. With this notation we have the following (sufficient) condition which ensures that the scroll is physically feasible.

THEOREM 5.1. *If $\varphi_s \geq 2\pi$, $\delta \leq \varrho(0)$, and*

$$(5.2) \quad (\bar{\mathbf{x}}(\varphi) - \tilde{\mathbf{y}}(\varphi)) \cdot \mathbf{f}(\varphi) \geq r + 2\delta \quad \text{for all } \varphi \in [-\pi, \varphi_s - \pi],$$

then

$$(5.3) \quad d(\tilde{\mathbf{x}}, \mathbf{y}) \geq d(\bar{\mathbf{x}}, \bar{\mathbf{y}}) \geq r,$$

$$(5.4) \quad d(\tilde{\mathbf{x}}, \bar{\mathbf{y}}) = d(\bar{\mathbf{x}}, \mathbf{y}) = r,$$

$$(5.5) \quad d(\mathbf{y}, \tilde{\mathbf{y}}) = d(\mathbf{x}, \tilde{\mathbf{x}}) \geq 2\delta,$$

where $d(\cdot, \cdot)$ denotes the distance between two curves.

The inequality (5.5) ensures that as described above we can “fatten” \mathbf{x} on the inside to have thickness 2δ without colliding with $\tilde{\mathbf{x}}$. The inequalities (5.3) and (5.4) ensure that the scroll can orbit freely in a circle with radius r .

Proof. By symmetry we have $d(\tilde{\mathbf{x}}, \mathbf{y}) = d(\mathbf{x}, \tilde{\mathbf{y}}) \geq d(\bar{\mathbf{x}}, \bar{\mathbf{y}})$. So to prove (5.3) we only have to show that $d(\bar{\mathbf{x}}, \bar{\mathbf{y}}) \geq r$. We first show that

$$(5.6) \quad \bar{\mathbf{x}}([- \varphi - 2\pi, \varphi + \pi]) \subseteq H_{\bar{\mathbf{x}}, \varphi} \quad \text{for } \varphi \in [-\pi, \varphi_s - \pi].$$

By Lemma 2.3 (cf. Remark 2.5) we have $\bar{\mathbf{x}}([- \pi, \varphi + \pi]) \subseteq H_{\bar{\mathbf{x}}, \varphi}$. So let us consider $\varphi' \in [-\varphi - 2\pi, -\pi]$ and put $\varphi'' = -\varphi' - \pi \in [0, \varphi + \pi]$. If $\varphi \geq 0$, then, as $\delta \leq \varrho(0)$, we can once more use Lemma 2.3 and obtain

$$\bar{\mathbf{x}}(\varphi') = \mathbf{x}_\delta(\varphi'') \in H_{\mathbf{x}_\delta, \varphi} \subseteq H_{\mathbf{x}, \varphi},$$

so (5.6) holds. If $\varphi \in [-\pi, 0]$, then $\mathbf{f}(\varphi) \cdot \mathbf{e}(\tau) > 0$ for $\tau \in [0, \varphi + \pi]$, so

$$\mathbf{f}(\varphi) \cdot \int_0^{\varphi''} (\varrho(\tau) - 2\delta) \mathbf{e}(\tau) d\tau > 0.$$

As the endpoint $\mathbf{x}_\delta(0)$ of the half-circle clearly is contained in the supporting half-plane, we have $\bar{\mathbf{x}}(\varphi') = \mathbf{x}_\delta(\varphi'') = \mathbf{x}_\delta(0) + \int_0^{\varphi''} (\varrho(\tau) - 2\delta) \mathbf{e}(\tau) d\tau \in H_{\bar{\mathbf{x}}, \varphi}$, and (5.6) holds in this case too; see Figure 5.2. We have now established (5.6). As $H_{\mathbf{x}, \varphi} \subseteq H_{\tilde{\mathbf{y}}, \varphi} \subseteq H_{\bar{\mathbf{y}}, \varphi}$, or equivalently $H_{\bar{\mathbf{x}}, \varphi} \subseteq H_{\bar{\mathbf{y}}, -\varphi - 3\pi} \subseteq H_{\bar{\mathbf{y}}, \varphi}$, we have for $\varphi \in [-\pi, \varphi_s - \pi]$ that

$$d(\bar{\mathbf{y}}(\varphi), \bar{\mathbf{x}}([- \varphi - 2\pi, \varphi + \pi])) \geq (\mathbf{x}(\varphi) - \tilde{\mathbf{y}}(\varphi)) \cdot \mathbf{f}(\varphi) \geq r + 2\delta,$$

$$d(\bar{\mathbf{y}}(-\varphi - 3\pi), \bar{\mathbf{x}}([- \varphi - 2\pi, \varphi + \pi])) \geq (\mathbf{x}(\varphi) - \tilde{\mathbf{y}}(\varphi) - 2\delta \mathbf{f}(\varphi)) \cdot \mathbf{f}(\varphi) \geq r.$$

Using the symmetry, we have all in all that

$$(5.7) \quad d(\bar{\mathbf{y}}(\varphi), \bar{\mathbf{x}}([- \varphi - 2\pi, \varphi + \pi])) \geq r + 2\delta \quad \text{for } \varphi \geq -\pi,$$

$$d(\bar{\mathbf{y}}(\varphi), \bar{\mathbf{x}}([\varphi - \pi, -\varphi - 2\pi])) \geq r \quad \text{for } \varphi \leq -2\pi,$$

$$(5.8) \quad d(\bar{\mathbf{x}}(\varphi), \bar{\mathbf{y}}([- \varphi - 3\pi, \varphi - \pi])) \geq r + 2\delta \quad \text{for } \varphi \geq 0,$$

$$d(\bar{\mathbf{x}}(\varphi), \bar{\mathbf{y}}([\varphi - 3\pi, \varphi - 2\pi])) \geq r \quad \text{for } \varphi \leq -\pi.$$

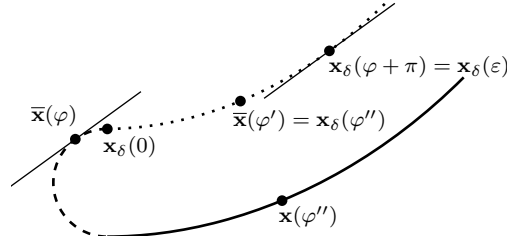


Fig. 5.2 If $\varphi = \varepsilon - \pi \in [-\pi, 0]$, then $\mathbf{x}_\delta(\varphi'') \in H_{\bar{\mathbf{x}}, \varphi}$ for $0 \leq \varphi'' \leq \varepsilon$.

We have shown that $|\bar{\mathbf{x}}(\varphi_1) - \bar{\mathbf{y}}(\varphi_2)| \geq r$ for $(\varphi_1, \varphi_2) \notin [-\pi, 0] \times [-2\pi, -\pi]$. So let us now assume the opposite: we consider points on the two half-circles attached to the ends. As $(\bar{\mathbf{x}}(-\pi) - \bar{\mathbf{y}}(-\pi)) \cdot \mathbf{f}(-\pi) \geq r + 2\delta$ the distance between the center of the half-circles satisfies

$$|(\bar{\mathbf{x}}(-\pi) + \delta \mathbf{f}(-\pi)) - (\bar{\mathbf{y}}(-\pi) + \delta \mathbf{f}(-\pi))| \geq (\bar{\mathbf{x}}(-\pi) - \bar{\mathbf{y}}(-\pi)) \cdot \mathbf{f}(-\pi) \geq r + 2\delta.$$

As the radius of both half-circles is δ , the distance between the half-circles is greater than r . This completes the proof of (5.3).

The first equality in (5.4) is due to the symmetry. For the second we first observe that $\mathbf{y}(\varphi) = \mathbf{x}(\varphi) - r\mathbf{f}(\varphi)$. Hence we have that $d(\bar{\mathbf{x}}, \mathbf{y}) \leq r$, and we need only to show that $d(\bar{\mathbf{x}}, \mathbf{y}) \geq r$. By the same reasoning as above we see that

$$d(\mathbf{y}(\varphi), \bar{\mathbf{x}}([- \varphi - 2\pi, \varphi + \pi])) \geq d(\mathbf{y}(\varphi), \mathbf{x}(\varphi)) = r.$$

By symmetry, (5.2) implies that

$$(\tilde{\mathbf{y}}(\varphi) - \mathbf{x}(\varphi + 2\pi)) \cdot \mathbf{f}(\varphi) \geq r + 2\delta \quad \text{for all } \varphi \in [-2\pi, \varphi_s - 2\pi].$$

For $\varphi \in [-\pi, \varphi_s - 2\pi]$ we now have that

$$(\mathbf{x}(\varphi) - \mathbf{x}(\varphi + 2\pi)) \cdot \mathbf{f}(\varphi) = (\mathbf{x}(\varphi) - \tilde{\mathbf{y}}(\varphi) + \tilde{\mathbf{y}}(\varphi) - \mathbf{x}(\varphi + 2\pi)) \cdot \mathbf{f}(\varphi) \geq 2(r + \delta).$$

So if $\varphi \in [2\pi, \varphi_s]$, then

$$\begin{aligned} d(\bar{\mathbf{x}}(\varphi), \mathbf{y}([0, \varphi - \pi])) &\geq d(\mathbf{x}(\varphi), \mathbf{y}(\varphi - 2\pi)) \geq (\mathbf{y}(\varphi - 2\pi) - \mathbf{x}(\varphi)) \cdot \mathbf{f}(\varphi) \\ &= (\mathbf{x}(\varphi - 2\pi) - r\mathbf{f}(\varphi) - \mathbf{x}(\varphi)) \cdot \mathbf{f}(\varphi) \geq r + 4\delta. \end{aligned}$$

If $\varphi \in [-\varphi_s - \pi, -3\pi]$, then $\bar{\mathbf{x}}(\varphi) = \mathbf{x}_\delta(-\varphi - \pi) = \mathbf{x}(-\varphi - \pi) - 2\delta\mathbf{f}(-\varphi)$, and hence

$$d(\bar{\mathbf{x}}(\varphi), \mathbf{y}([0, -\varphi - 2\pi])) \geq r + 2\delta.$$

We are only missing $|\bar{\mathbf{x}}(\varphi_1) - \mathbf{y}(\varphi_2)|$, where $0 \leq \varphi_2 \leq \varphi_1 - \pi$ and $\pi \leq \varphi_1 \leq 2\pi$ or where $0 \leq \varphi_2 \leq -\varphi_1 - 3\pi$ and $-3\pi \leq \varphi_1 \leq -2\pi$. So let $\varphi_2 \in [0, \pi]$ and consider first the function $\varphi_1 \mapsto |\bar{\mathbf{x}}(\varphi_1) - \mathbf{y}(\varphi_2)|$ for $\pi \leq \varphi_1 \leq 2\pi$. The values at the endpoints are greater than r so we need only to consider the stationary points. These are points with parallel tangents, i.e., $\varphi_1 = \varphi_2 + \pi$. For such a point we have

$$\begin{aligned} |\bar{\mathbf{x}}(\varphi_2 + \pi) - \mathbf{y}(\varphi_2)| &\geq (\mathbf{y}(\varphi_2) - \bar{\mathbf{x}}(\varphi_2 + \pi)) \cdot \mathbf{f}(\varphi_2 + \pi) \\ &= (\mathbf{x}(\varphi_2) - r\mathbf{f}(\varphi_2) - \bar{\mathbf{x}}(\varphi_2 + \pi)) \cdot \mathbf{f}(\varphi_2 + \pi) \\ &= (\mathbf{x}(\varphi_2 + \pi) - \bar{\mathbf{x}}(\varphi_2) + r\mathbf{f}(\varphi_2)) \cdot \mathbf{f}(\varphi_2) \geq r, \end{aligned}$$

where we have used Lemma 2.4 for the last inequality. The case with $-3\pi \leq \varphi_1 \leq -2\pi$ is similar, and this completes the proof of (5.4). We are left with (5.5), but by (5.7) and (5.8) we have $|\mathbf{x}(\varphi) - \tilde{\mathbf{y}}(\varphi')| \geq r + 2\delta$ if $\varphi > 0$ and $\varphi' > -\pi$. Thus

$$|\mathbf{x}(\varphi) - \tilde{\mathbf{x}}(\varphi')| \geq |\mathbf{x}(\varphi) - \tilde{\mathbf{y}}(\varphi')| - |\tilde{\mathbf{y}}(\varphi') - \tilde{\mathbf{x}}(\varphi')| \geq r + 2\delta - r = 2\delta.$$

The first equality in (5.5) is once more due to symmetry. \square

The importance of Theorem 5.1 is that it enable us to replace the potentially very difficult task of checking whether several curves intersect with the easier task of checking the sign of the single univariate function.

6. Examples. For the circle involute the derivative ϱ' of the radius of curvature is a constant, and we will now perturb the circle involute in the following simple way. We consider $\varphi \in [0, 6\pi]$; i.e., we have three turns of the spiral, and we change the constant ϱ' by adding a constant in the middle interval $[2\pi, 4\pi]$. To be precise, we consider the piecewise constant function

$$\frac{d\varrho}{d\varphi} = \begin{cases} \frac{r + 2\delta}{\pi}, & \varphi \in [0, 6\pi] \setminus [2\pi, 4\pi], \\ \frac{r + 2\delta + h}{\pi}, & \varphi \in [2\pi, 4\pi], \end{cases}$$

$$\varrho = \varrho_0 + \int_0^\varphi \frac{d\varrho}{d\varphi} d\varphi, \quad \text{and} \quad \mathbf{x} = \left(\frac{r + \delta}{\pi}, -\varrho_0 \right) + \int_0^\varphi \varrho \mathbf{e} d\varphi.$$

With this choice we increase the compression on the second turn, and this is advantageous with respect to leakage; cf. [6]. We reflect in $(0, 0)$, i.e., we put $\tilde{\mathbf{y}}(\varphi) = -\mathbf{x}(\varphi + \pi)$. This point, or rather $\mathbf{x}(0)$, is chosen such that the inner turn of the compressor is the same as the standard circle involute scroll compressor. As described in section 5 we extend \mathbf{x} to give the curve $\bar{\mathbf{x}}$ by attaching a small half-circle with radius δ to $\mathbf{x}(0)$. We now apply Theorem 5.1 to ensure the physical feasibility of the scroll. The condition (5.2) says that the function $f(\varphi) = (\bar{\mathbf{x}}(\varphi) - \tilde{\mathbf{y}}(\varphi)) \cdot \mathbf{f}(\varphi) - (r + 2\delta)$ has to be nonnegative. If $\varphi \geq 0$ and hence $\bar{\mathbf{x}}(\varphi) = \mathbf{x}(\varphi)$, this is easily seen to be the case, but in the interval $[-\pi, 0]$ we have

$$f(\varphi) = (\varrho_0 - \delta)(1 - \cos \varphi) + \frac{1}{\pi}(r + 2\delta)(\varphi - \sin \varphi).$$

The last term is negative in the given interval, so if $\delta = \varrho_0$, then f becomes negative; but if $\delta < \varrho_0$, then $f'(0) = 0$, $f''(0) < 0$, and $f'(\varphi)$ has at most a single zero in the interval $[-\pi, 0)$, so we need only consider the point $\varphi = -\pi$. That is, f is positive if and only if $f(-\pi) = 2(\varrho_0 - \delta) - (r + 2\delta) \geq 0$ or

$$(6.1) \quad \varrho_0 \geq 2\delta + \frac{r}{2}.$$

Besides (5.2), we have the condition $\delta \leq \varrho_0$, but it is now vacuous. Half the diameter of the compressor is approximately

$$(6.2) \quad R = \frac{1}{2}(\mathbf{x}(5\pi) - \mathbf{x}(6\pi)) \cdot \mathbf{f}(0) = \frac{11}{2}r + \varrho_0 + 11\delta + 2h,$$

and if we isolate ϱ_0 from (6.2) we get

$$\varrho_0 = R - \frac{11}{2}r - 11\delta - 2h.$$

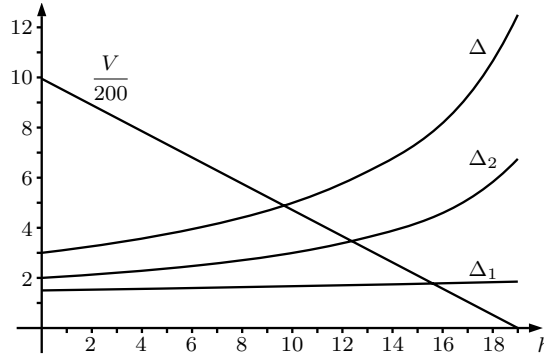


Fig. 6.1 The compressions Δ_1 , Δ_2 , Δ , and the choke volume V .

Inserting this in (6.1) we get the equivalent condition,

$$(6.3) \quad 6r + 2h \leq R - 13\delta.$$

From (3.1) we obtain

$$\mathcal{A}(0) = \pi r(3r + 2\rho_0 + 4\delta) = 2\pi r(R - 4r - 9\delta - 2h),$$

$$\mathcal{A}(2\pi) = \pi r(7r + 2\rho_0 + 12\delta + 2h) = 2\pi r(R - 2r - 5\delta - h),$$

$$\mathcal{A}(4\pi) = \pi r(11r + 2\rho_0 + 20\delta + 4h) = 2\pi r(R - \delta).$$

The compression and the choke volume are given by

$$\Delta_1 = \frac{R - \delta}{R - 2r - 5\delta - h}, \quad \Delta_2 = \frac{R - 2r - 5\delta - h}{R - 4r - 9\delta - 2h},$$

$$\Delta = \frac{R - \delta}{R - 4r - 9\delta - 2h}, \quad V = 2\pi r(d - \delta).$$

Increasing r and h increases both the compression and the choke volume, so considering (6.3), we put $6r + 2h = R - 13\delta$ or

$$r = \frac{R - 13\delta - 2h}{6},$$

from which we get

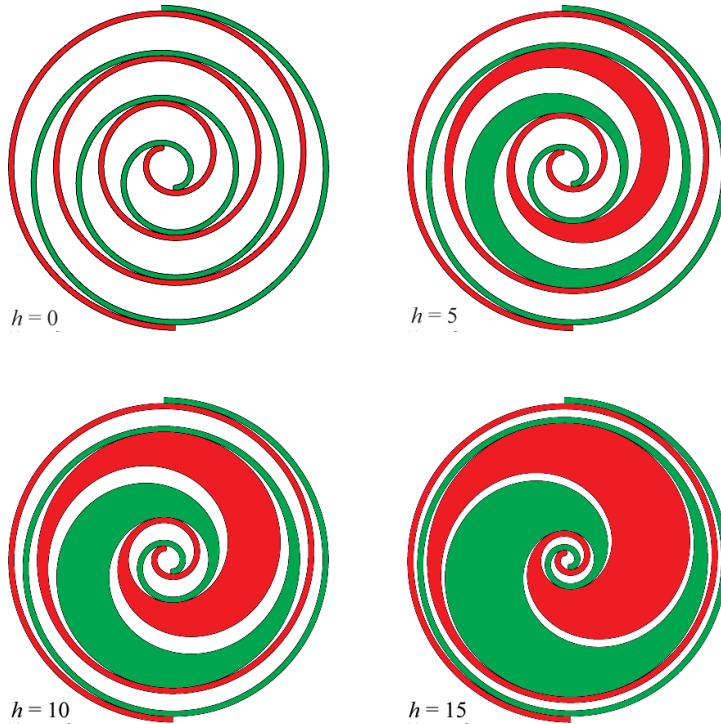
$$\Delta_1 = \frac{3(R - \delta)}{2R - 2\delta - h}, \quad \Delta_2 = \frac{2R - 2\delta - h}{R - \delta - 2h},$$

$$\Delta = \frac{3(R - \delta)}{R - \delta - 2h}, \quad V = \frac{\pi(R - 13\delta - 2h)(R - \delta)}{3}.$$

We look at the case $R = 51$ and $\delta = 1$. Then we have $h \leq 19$, and the compressions and the choke volume plotted in Figure 6.1. We now look closer at the cases $h = 0, 5, 10, 15$. The geometric properties of the three scroll compressors are summarized in Table 6.1 and the scrolls are plotted in Figure 6.2.

Table 6.1 The key geometric parameters for the four designs.

h	r	ϱ_0	Δ_1	Δ_2	Δ	V
0	6.33	5.17	1.50	2.00	3.00	1990
5	4.67	4.33	1.58	2.38	3.75	1466
10	3.00	3.50	1.67	3.00	5.00	942
15	1.33	2.67	1.76	4.25	7.50	419

**Fig. 6.2** The standard circle involute scroll compressors ($h = 0$) and three variations.

We started with four design parameters, essentially the size R , the minimal thickness δ , the radius of the orbit r , and the jump h in ϱ' . The size and thickness will in practice be given a priori, so we are left with r and h . In a practical application one would use a more general form of the function ϱ , and besides the minimal thickness δ and the overall size R , the compression Δ would probably be given. The optimal design would then be the one that maximizes the choke volume. Equivalently, the choke volume could be given too, and then the overall size R would be minimized. In our case the simple analytical expressions for the geometric properties allowed us to perform the “optimization” exactly, and we ended up with just one parameter h we could vary to obtain scrolls with different compressions and “optimal” choke volume.

In a realistic design process an important parameter is the *leakage*. We will just mention that it can be shown that if we ignore the leakage at the top and bottom, then the total leakage is proportional to

$$\int_0^{2\pi} \sqrt{\frac{1}{\varrho_y} - \frac{1}{\varrho_x} \left(\frac{V_0}{V_1}\right)} \left[\left(\frac{V_0}{V_1}\right)^\gamma - \left(\frac{V_1}{V_0}\right)^\gamma \right] dt,$$

where ϱ_x and ϱ_y are evaluated in $8\pi - t$, $V_0(t) = \mathcal{A}(6\pi - t)$, $V_1(t) = \mathcal{A}(4\pi - t)$, and γ is a coefficient depending on the fluid that is compressed; see [4] or [6]. Observe that the integrand can be evaluated in a closed analytical form. Having estimates for the leakage allows us to replace the “geometric” compression and choke volume in the optimization above with the physical compression and choke volume.

The scroll compressor has been the subject of a “mid-way project” at the Technical University of Denmark; see [1]. A part of the project is a web-based interactive “scroll designer” written in JAVA. The function ϱ can be an arbitrary piecewise linear function and is changed by adjusting the graph with the mouse. The program calculates the compression and choke volume and provides an animation of the resulting compressor.

7. Conclusion. We have shown how the use of the intrinsic equation of a planar curve allows us to calculate all interesting geometric characteristics of the scroll compressor in closed analytical form. This gives a sound and efficient foundation for an optimization process.

In order to understand the geometry of the scroll compressor, most of the classical constructions and concepts of the theory of planar curves have to be applied. It is from a didactic point of view especially appealing that the abstract notion of the intrinsic equation plays a key role in the modeling of a real life practical object. So the scroll compressor is an ideal example when teaching differential geometry; this aspect is addressed in [3].

Acknowledgments. We thank Danfoss A/S and, in particular, Stig Helmer Jørgensen for providing us with an interesting problem and answering many questions during the study group. We would also like to thank the other participants in the study group, in particular Peter Howell, for an inspiring week and many fruitful discussions.

REFERENCES

- [1] K. CHRISTENSEN, M. D. SØRENSEN, AND K. S. KRISTENSEN, *Modelling and Visualization of a Scroll Compressor*, mid-way project, Technical University of Denmark, 2000; also available at <http://www.mat.dtu.dk/student-projects/2000-scroll/>.
- [2] L. CREUX, *Rotary Engine*, U.S. Patent 801182, 1905.
- [3] J. GRAVESEN AND C. HENRIKSEN, *Geometrien af en scroll-kompressor. Fra et konkret problem til abstrakt matematik*, Normat, 47 (1999), pp. 1–19 (in Danish).
- [4] J. GRAVESEN, C. HENRIKSEN, AND P. HOWELL, *Danfoss: Scroll optimization*, in 32nd European Study Group with Industry, Final Report, J. Gravesen and P. Hjorth, eds., Department of Mathematics, Technical University of Denmark, Lyngby, 1998, pp. 3–35; also available at <http://www.mat.dtu.dk/ESG132/Report>.
- [5] H. W. GUGGENHEIMER, *Differential Geometry*, McGraw-Hill, New York, 1963.
- [6] P. HOWELL, *Fluid mechanical modelling of the scroll compressor*, in *Mathematical Modelling: Case Studies*, A. Fitt and E. Cumberbatch, eds., Cambridge University Press, Cambridge, UK, 1999.
- [7] J. McCULLOUGH AND F. HIRSCHFELD, *The scroll machine—an old principle with a new twist*, *Mech. Engrg.*, 101 (1979), pp. 46–51.